

Perturbed Angular Correlations

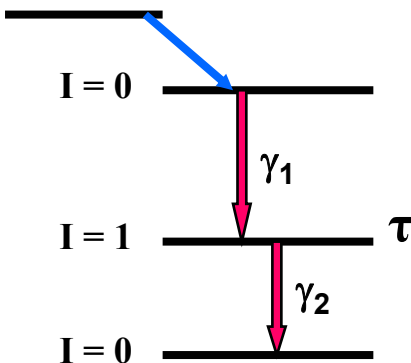
in nuclear physics and material science

- The phenomenon of γ - γ angular correlations
- Time Differential (TDPAC) and Time Integral (IPAC) technique
- Perturbation of Angular Correlations by Hyperfine Interactions
- Related techniques: TDPAD and SRPAC
- Applications
- Analysis of strengths and weaknesses
- Comparison with other hyperfine interaction techniques

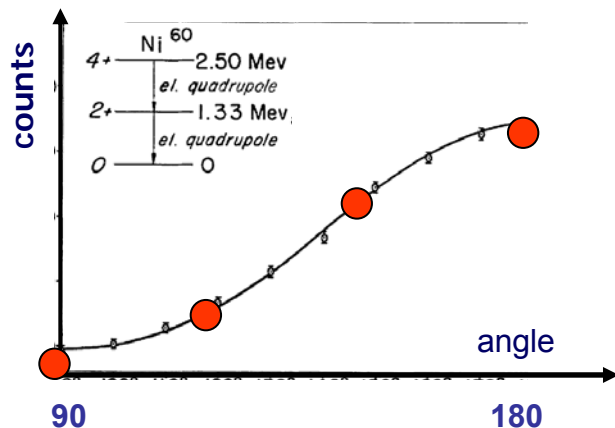
The phenomenon of unperturbed $\gamma - \gamma$ angular correlations

The time-integral mode (IPAC)

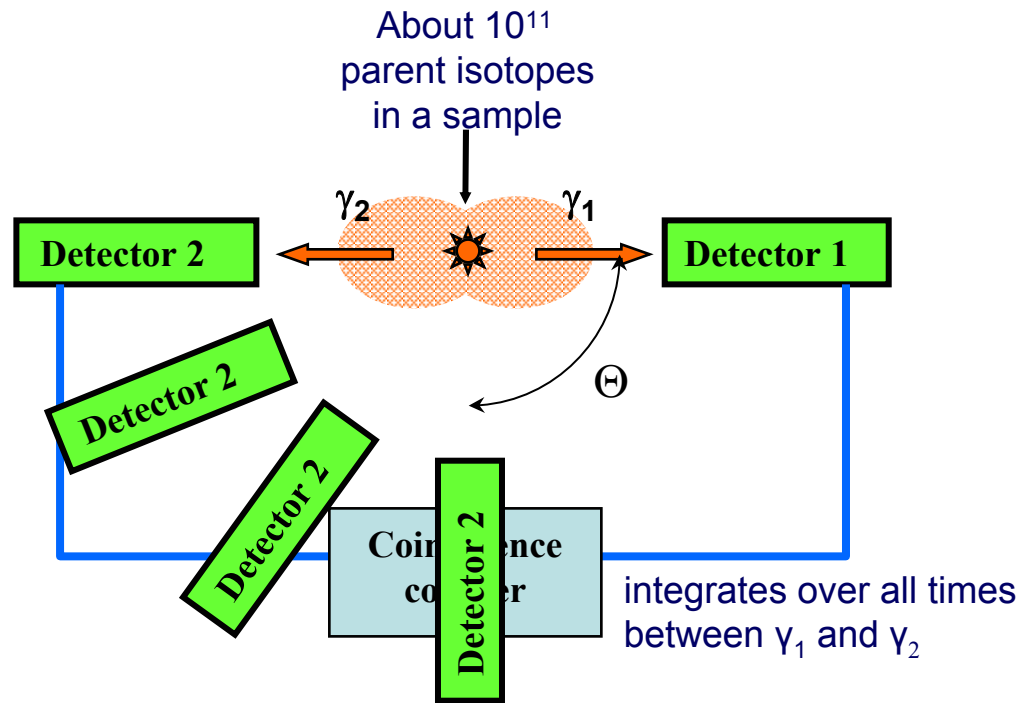
Parent isotope



For spin sequence 0-1-0:
counts $\approx \cos^2\Theta$



R.M. Steffen, Adv. In Phys. 4 (1955) 293

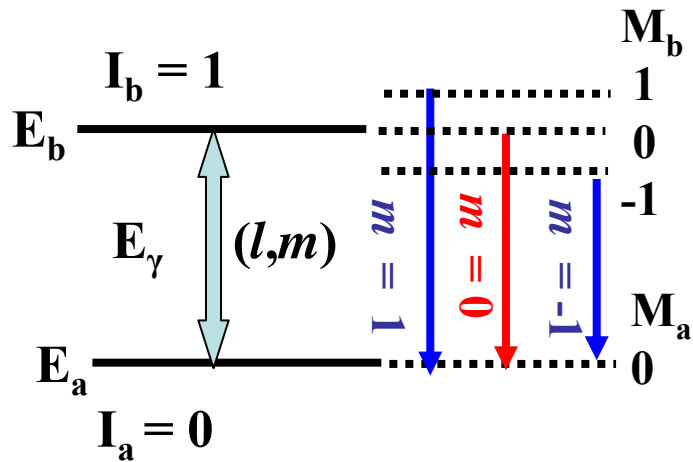


$$W(\Theta, t = 0 \rightarrow \infty) = 1 + A_{kk} P_k(\cos \Theta), \quad k = 2, 4$$

A_{kk} = angular correlation coefficients

depend on spins, parities and multipole order of the cascade

Gamma decay of excited nuclear states



Conservation of angular momentum:

$$|I_a - I_b| \leq l \leq |I_a + I_b|, \quad m = M_a - M_b$$

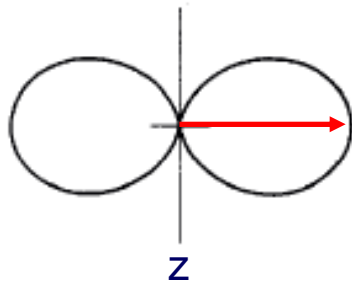
l : multipole order

$l = 1$ dipole radiation

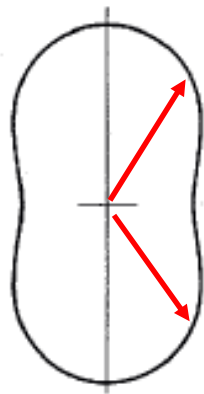
$l = 2$ quadrupole radiation

The angular characteristics $I_{l,m}(\Theta)$ of the gamma-radiation depends on (l, m)

dipole ($l=1$)

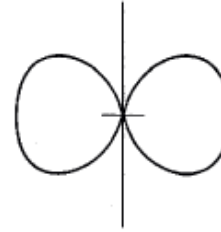


$l=1, m=0$

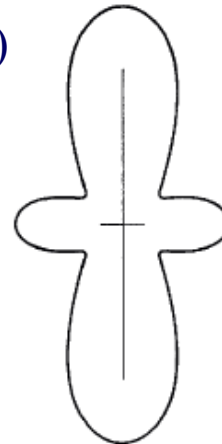


$l=1, m=\pm 1$

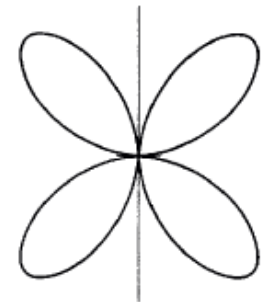
quadrupole ($l=2$)



$l=2, m=\pm 2$



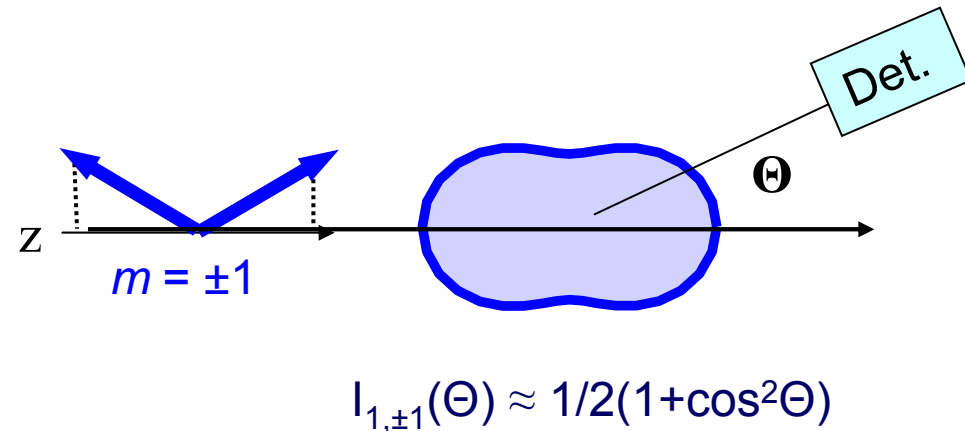
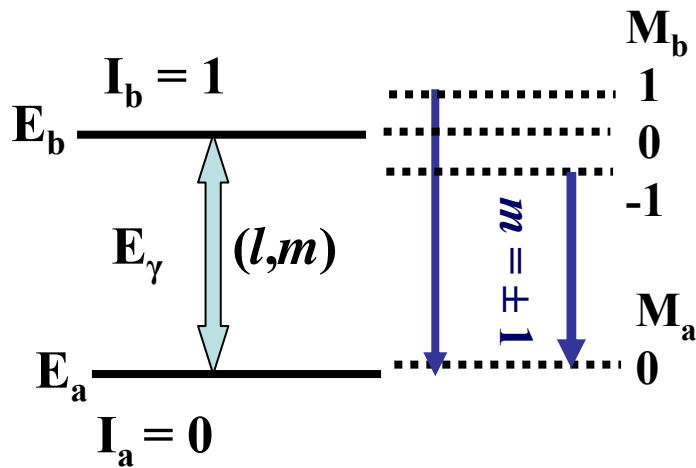
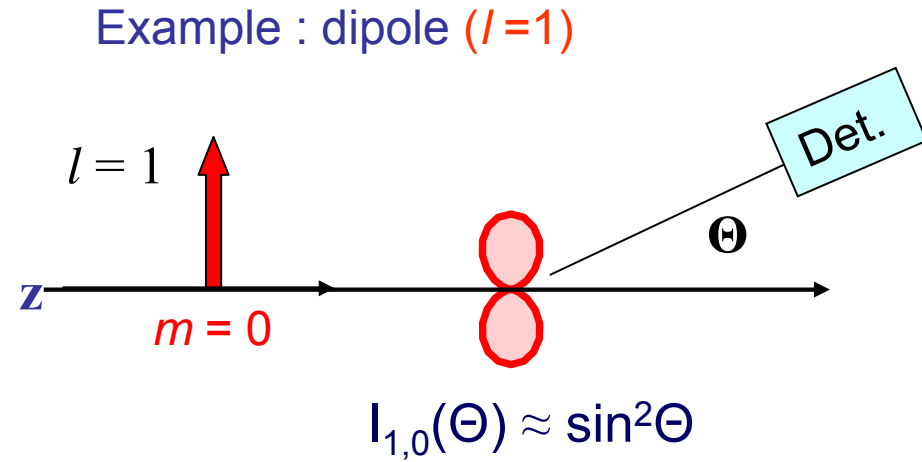
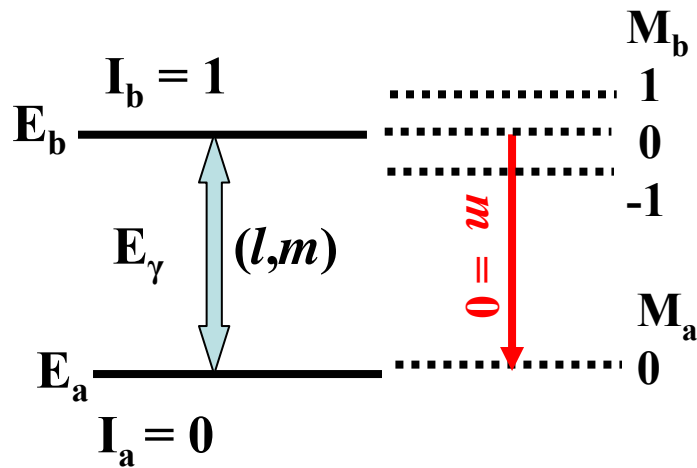
$l=2, m=\pm 1$



$l=2, m=\pm 0$

Nuclear physics : Determination of the multipole order and spins by measurement of $I_{l,m}(\Theta)$

Gamma emission from **aligned** nuclear states



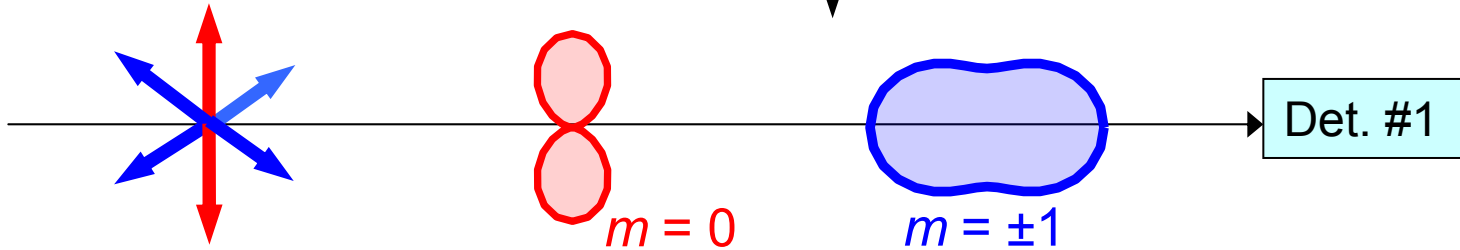
The radiation distribution informs on the spin orientation

Angular Correlations – Theoretical background

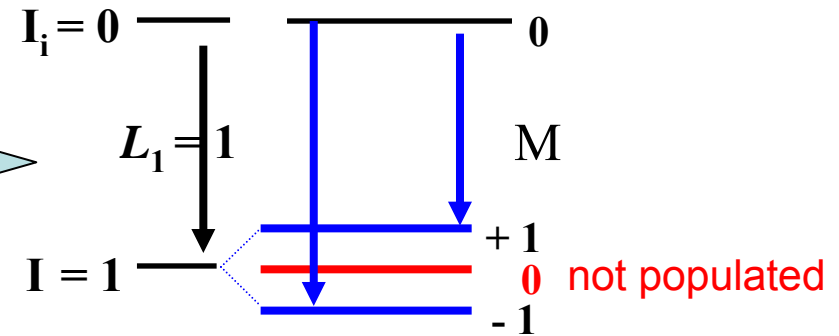
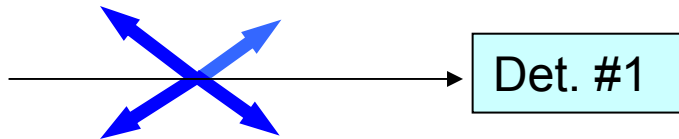
$$\begin{array}{c}
 \overline{\quad} \quad I_i = 0 \\
 L_1 \downarrow \gamma_1 \\
 \overline{\quad} \quad I = 1 \\
 L_2 \downarrow \gamma_2 \\
 \overline{\quad} \quad I_f = 0 \\
 ||_i^-|| \leq L_1 \leq ||_i^+ ||
 \end{array}$$

The first γ -transition with  I  L_1

Radiation emitted by an ensemble of randomly oriented nuclear spins:



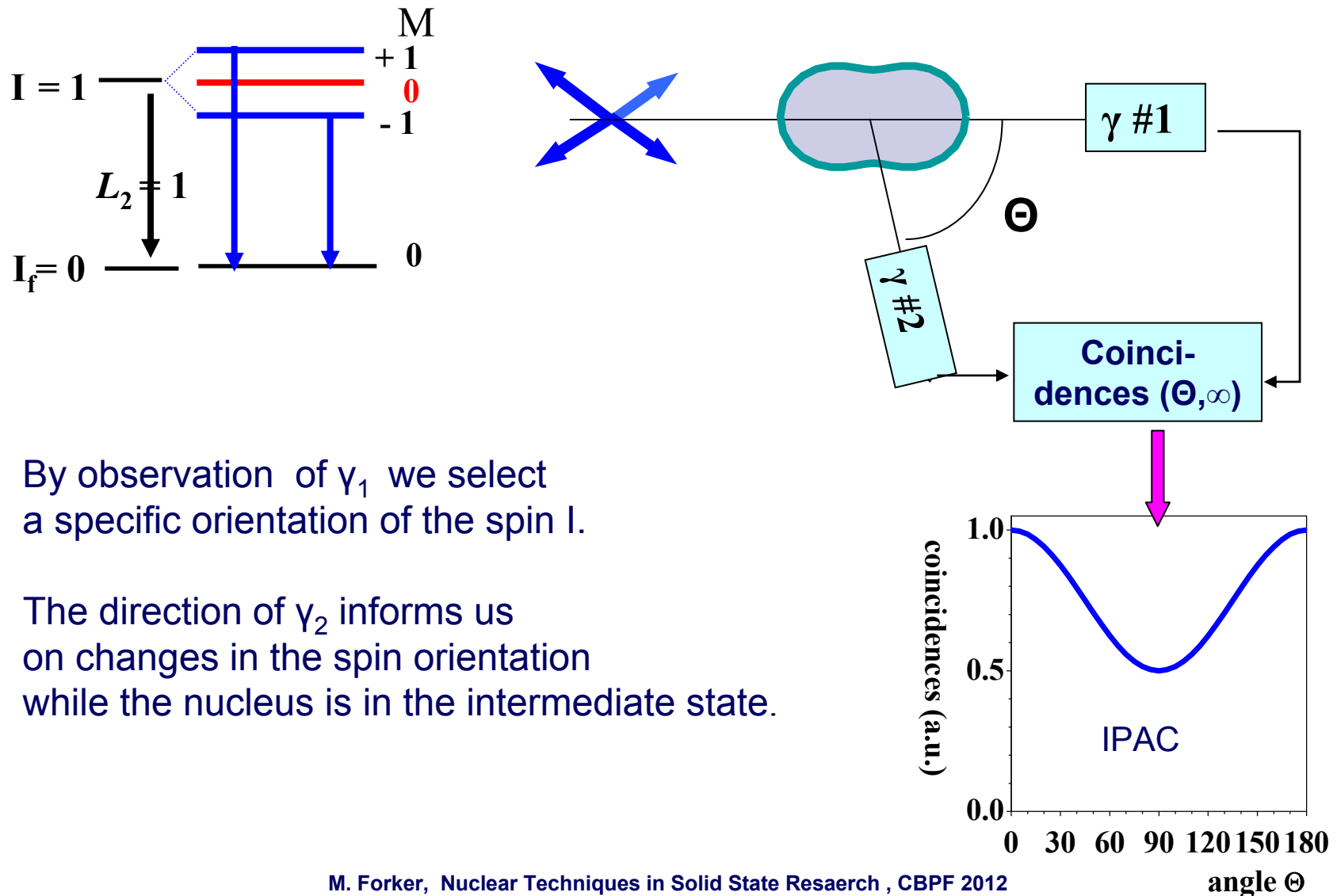
Nuclear spins seen by Det. #1



Observation of γ_1 = selection of a subgroup of spin orientations
Spin alignment !

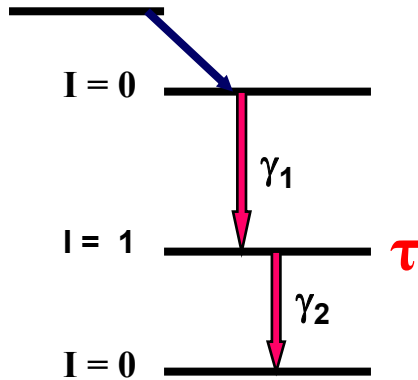
The **second** γ -transition of the $\gamma\gamma$ -cascade

Emission from an **aligned** spin ensemble

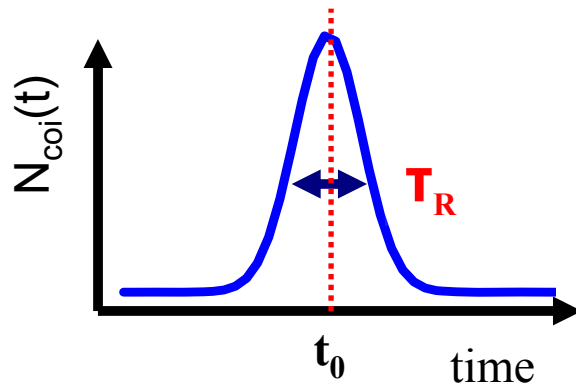


OBSERVATION MODES of Angular Correlations

Parent isotope



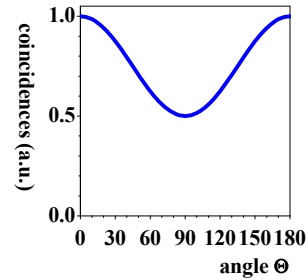
Time resolution



Time **integral** mode: **IPAC**

Half-width $T_R \geq$ life time τ

- Integration over all times of the intermediate state of the cascade
- Time-integrated observation of hyperfine interactions

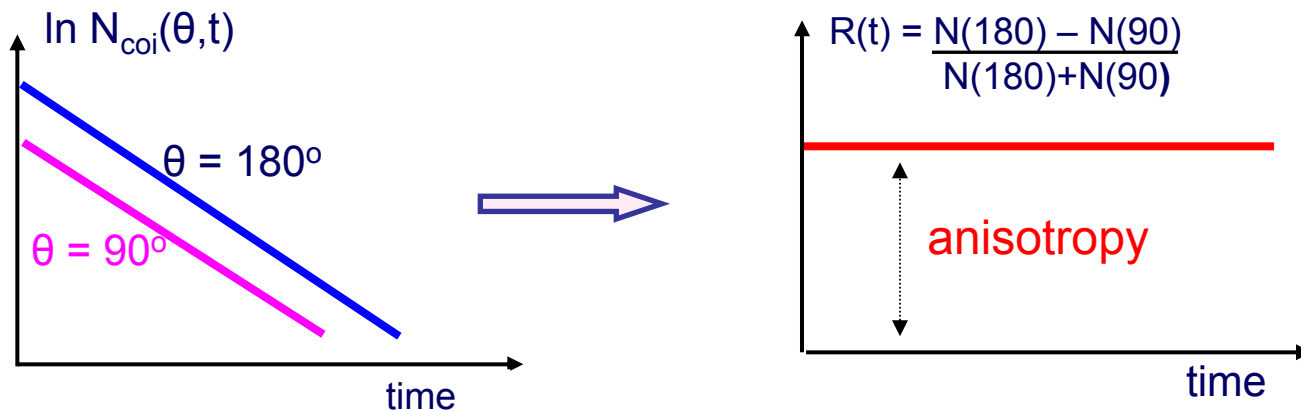
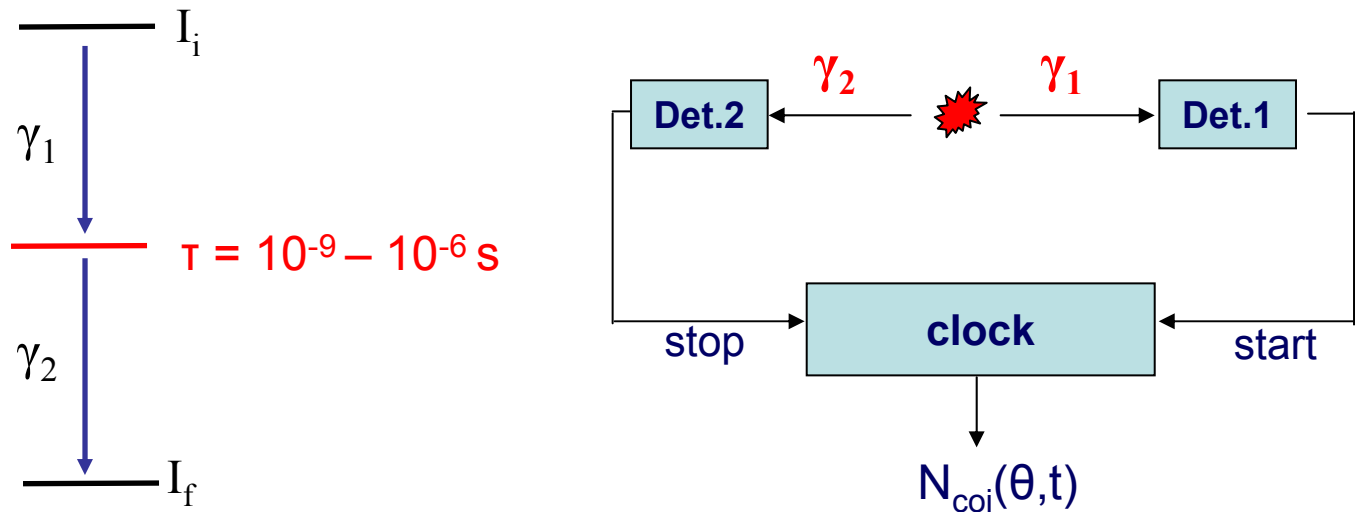


Time **differential** mode: **TDPAC**

Half-width $T_R \leq$ life time τ

- Measurement of the anisotropy as a function of the time the nucleus has spent in the intermediate state of the cascade
- Time resolved observation of hyperfine frequencies $\nu_L \leq 1/\Delta T$

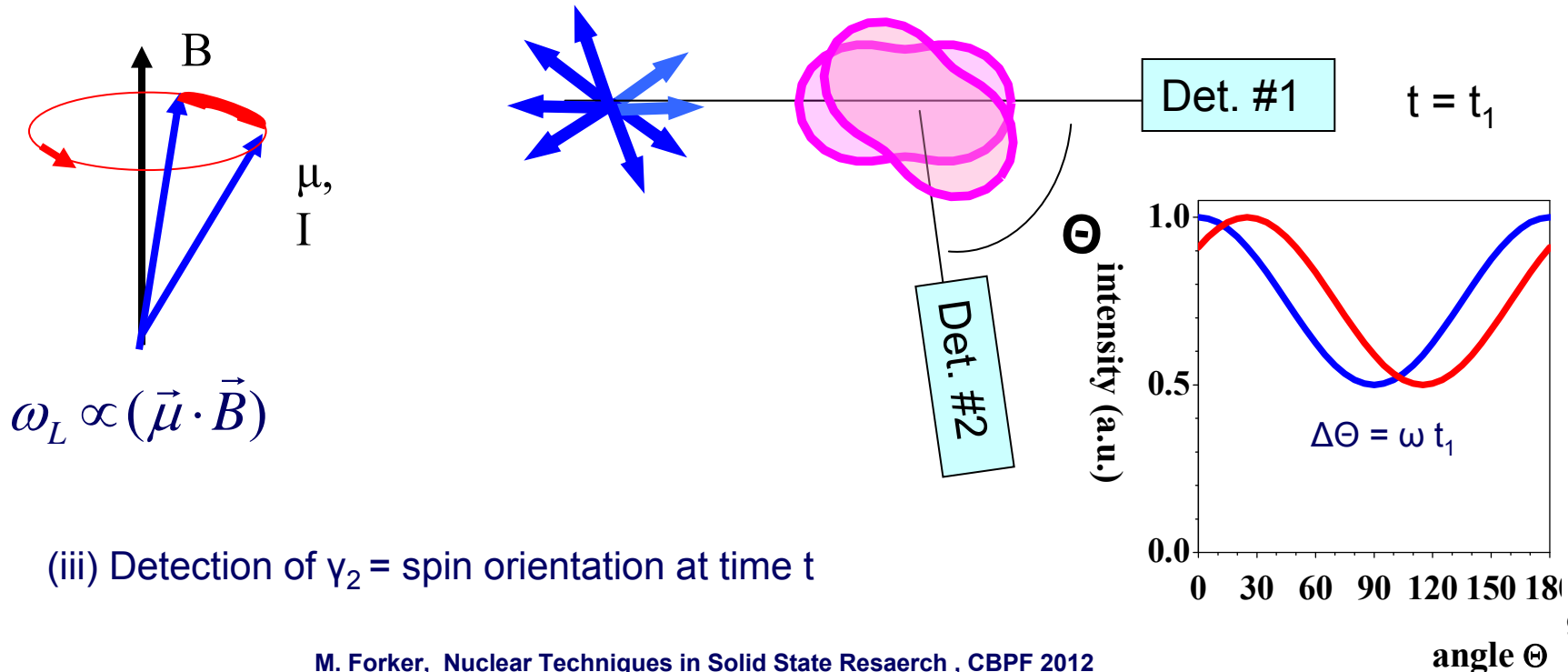
The time-differential mode (TDPAC) of unperturbed $\gamma - \gamma$ angular correlations



The **perturbation** of $\gamma\gamma$ angular correlations by hyperfine interactions

Basic aspects:

- (i) Detection of γ_1 = selection of a subgroup of spin orientations
 → anisotropic intensity distribution of γ_2
- (ii) Hyperfine interaction → Larmor precession of spins
 = Precession of the intensity distribution of γ_2

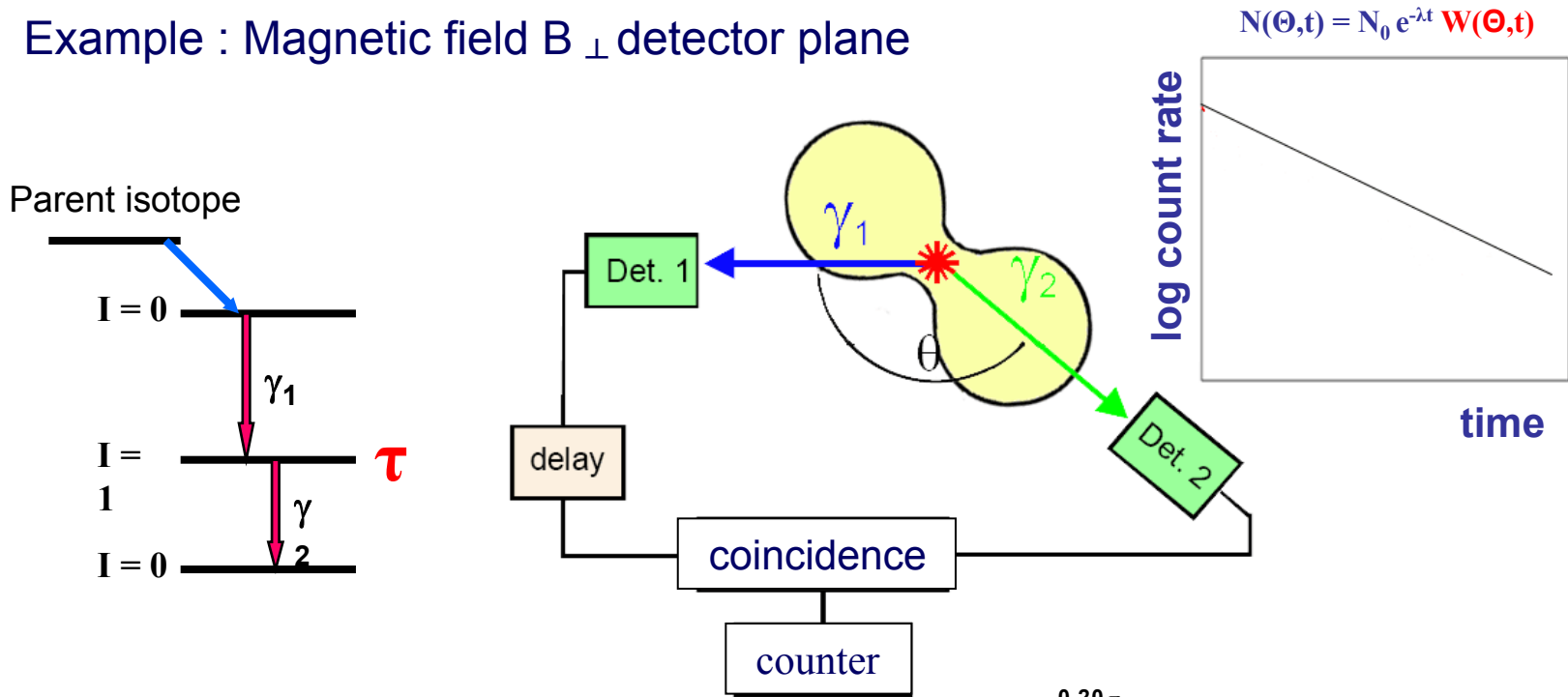


(iii) Detection of γ_2 = spin orientation at time t

The perturbation of $\gamma\gamma$ angular correlations by hyperfine interactions

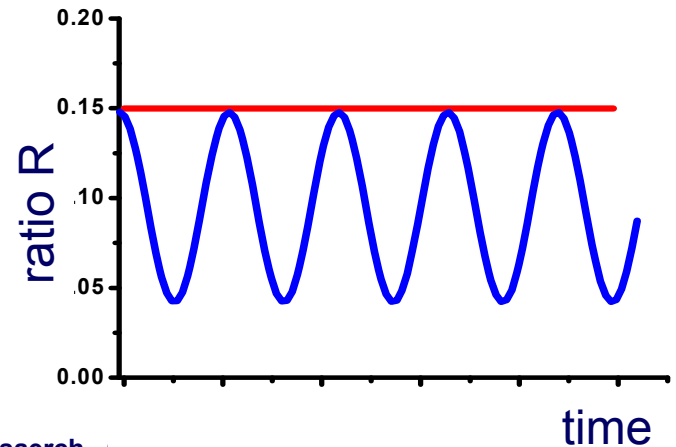
The time differential mode

Example : Magnetic field $B \perp$ detector plane



Elimination of the exponential decay

$$R(t) = \frac{N(180, t) - N(90, t)}{N(180, t) + N(90, t)}$$



Time differential Perturbed Angular Correlations – An Early Example (1965)

^{100}Rh in an external magnetic field of 0.22 T

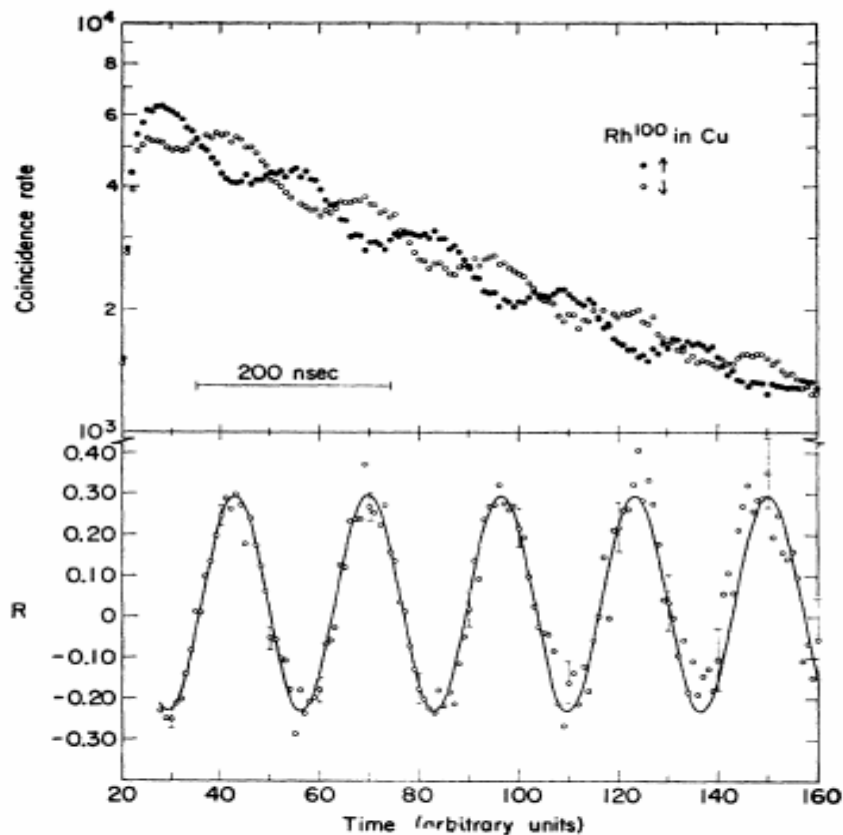


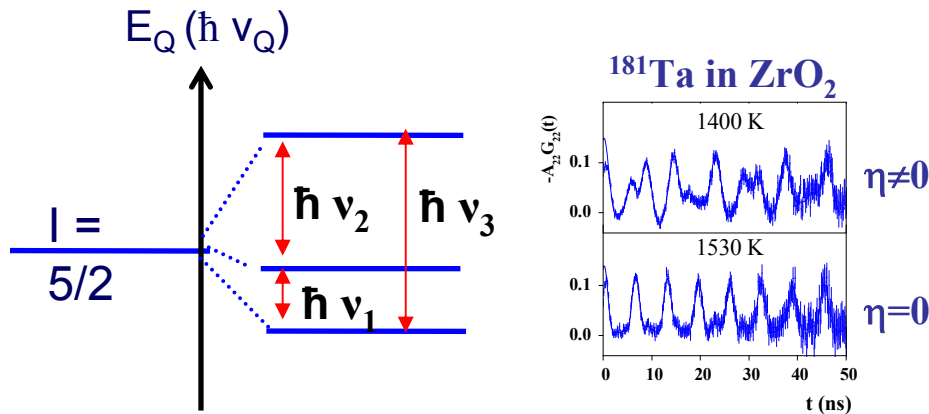
FIG. 4. Time-differential g -factor measurement with a source of Rh^{100} in copper in an external field of ± 2.22 kG. In the upper part of the figure the raw data of run No. 1 in Table II are shown without any background correction. In the lower part the corresponding ratios R_i are displayed. The full line represents the weighted least-squares fit to the data.

The perturbation of angular correlations by static hyperfine interactions

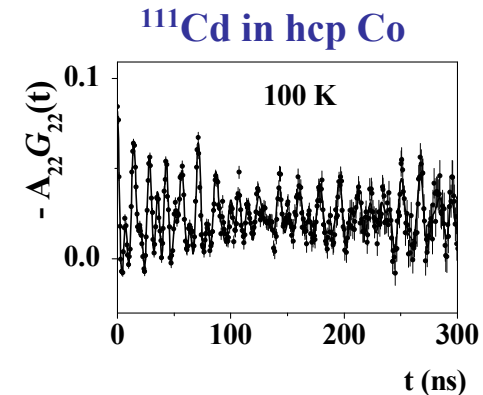
$$W(\theta, t) = \sum_{k=par} A_{kk} G_{kk}(t) P_k(\cos \theta)$$

$G_{kk}(t)$ = perturbation factor

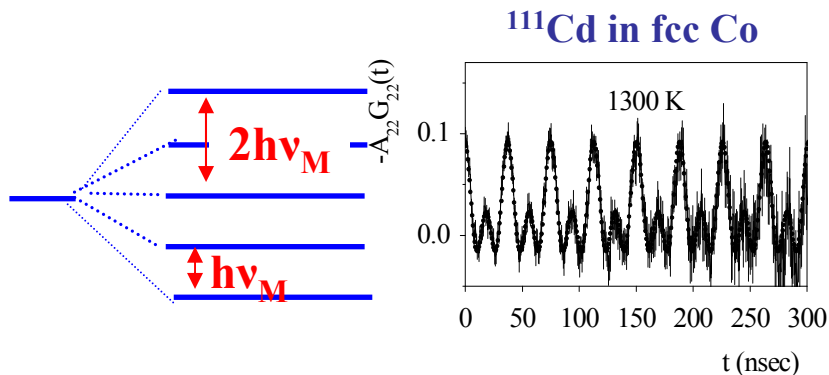
Electric quadrupole interaction



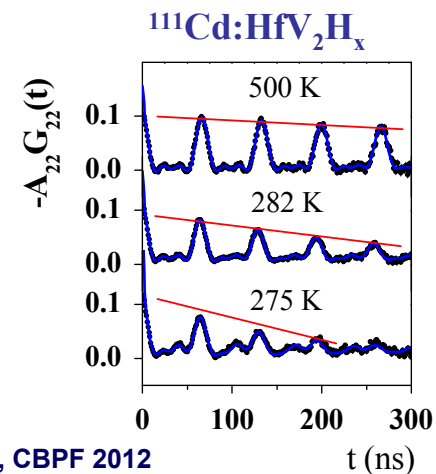
Combined MHFI + QI



Magnetic dipole interaction

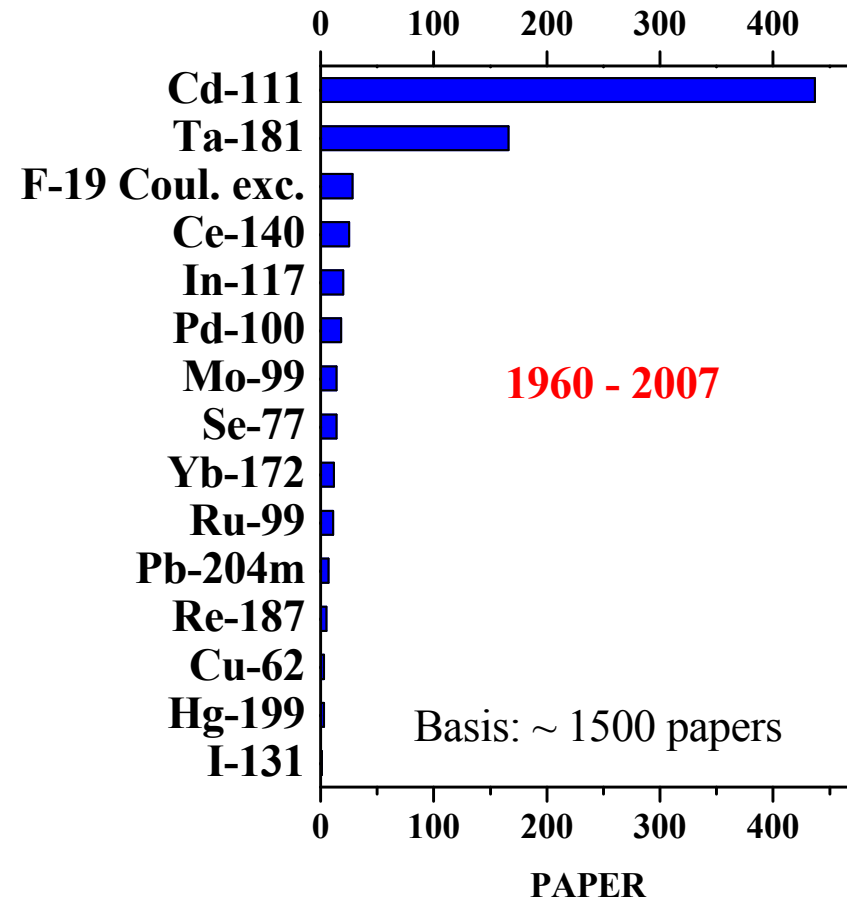


Dynamic QI



$\gamma\gamma$ -cascades for TDPAC measurements - required properties

- Mean life time τ of the intermediate state:
 $10^{-9} \text{ s} \leq \tau \leq 10^{-6} \text{ s}$
- Spin I of the intermediate state: $I \geq 1$
- Anisotropy: $A_{22} \geq 0.05$
- Intensity of the cascade
- Half- life of the mother isotope: $T_{1/2} \geq 1 \text{ h}$
(Laboratory experiments)
- Coincidence experiment:
data accumulation: 10 min to a few days

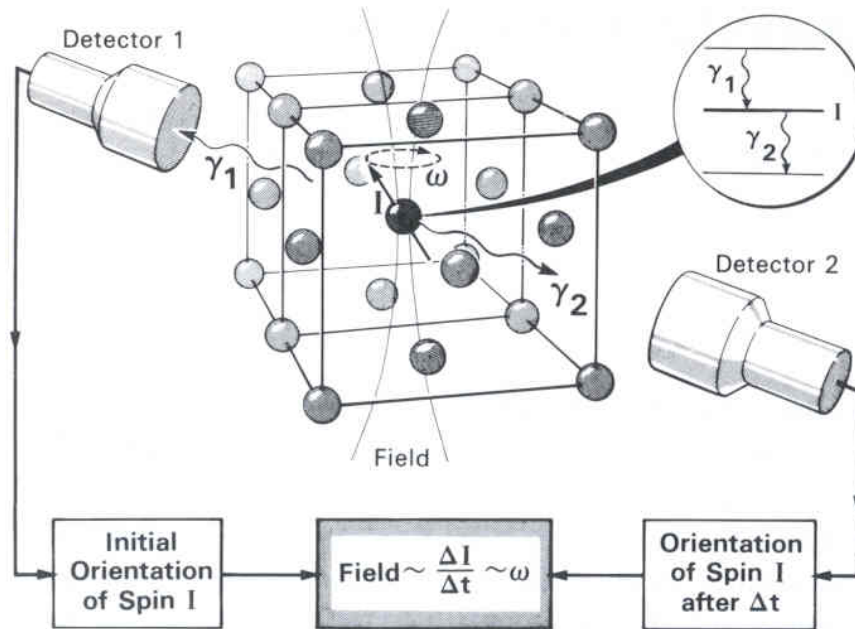


Number of suitable isotopes for laboratory experiments: ≤ 15

TDPAC spectrometer – basic aspects

Requirements:

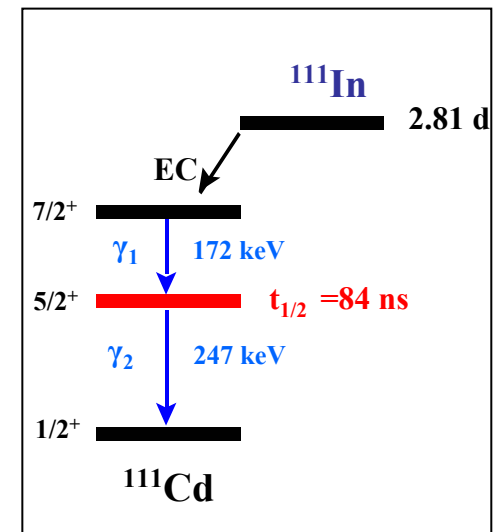
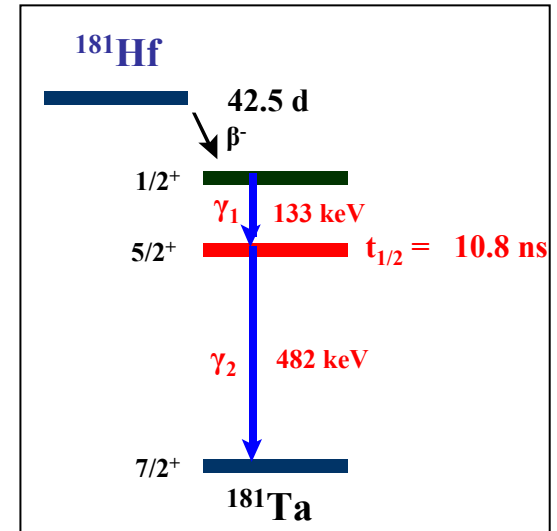
- high statistics
- high detection efficiency
- energy resolution
- time resolution



Present standard:

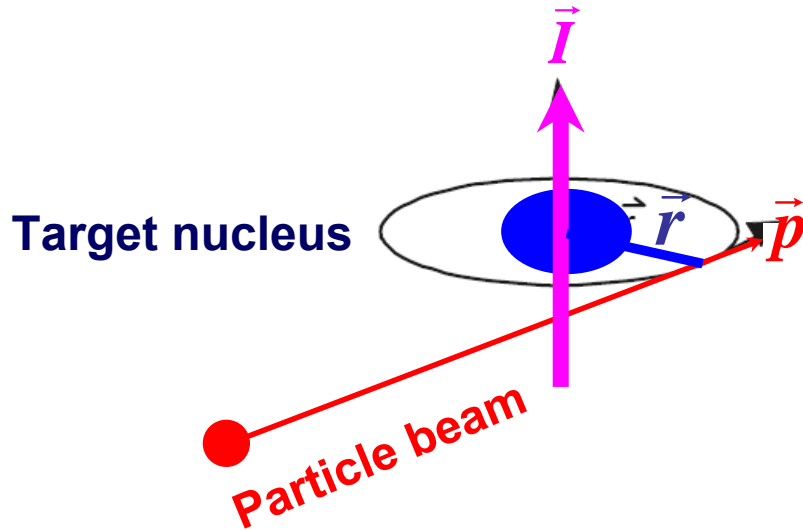
- Multi-detector arrays: up to 6 detectors
- Fast photomultiplier coupled to BaF₂ scintillators
- Time resolution: ~ 100 ps FWHM at ⁶⁰Co energies

popular isotopes



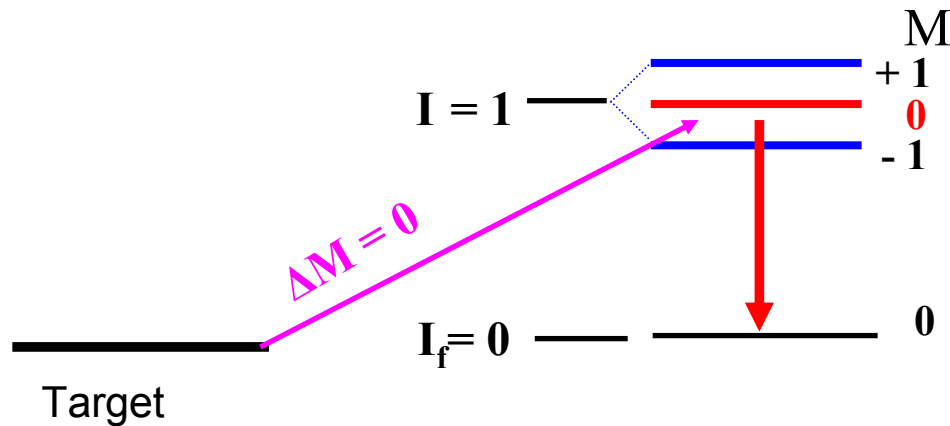
Perturbed angular **distribution** (TDPAD)

Production of spin alignment by nuclear reaction



In nuclear reaction the angular momentum transferred to the target nucleus is preferentially **perpendicular** to the beam axis

Nuclear reactions therefore favour $m = 0$ transitions, producing **aligned** nuclear states



The subsequent gamma-emission is **anisotropic**

Synchrotron radiation PAC (SRPAC)

Production of spin alignment by synchrotron radiation

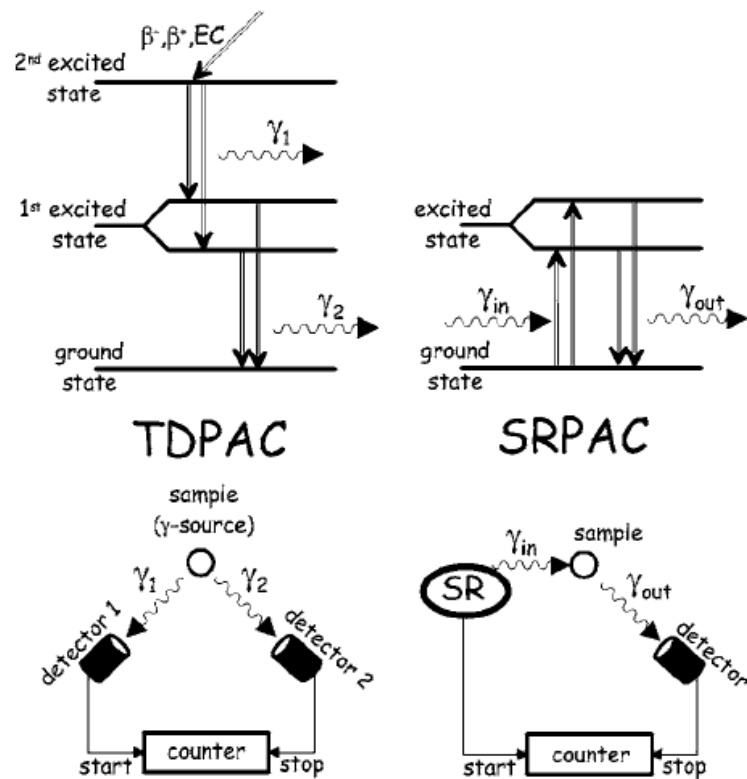


FIG. 1. Schemes of the principle and of the experimental setup for TDPAC (left side) and SRPAC (right side).

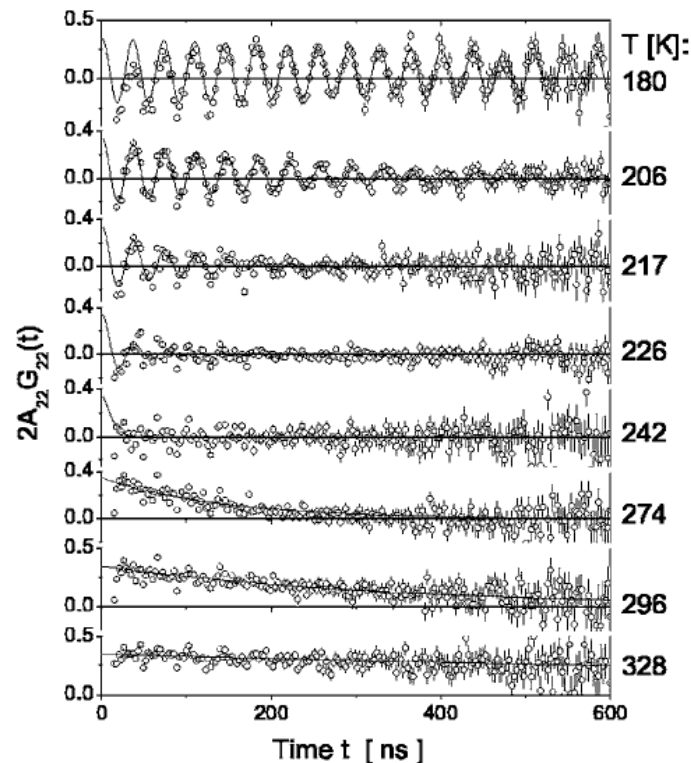
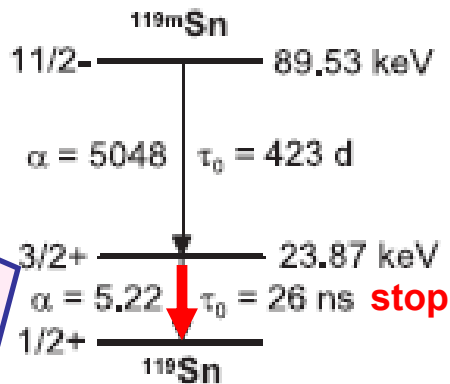
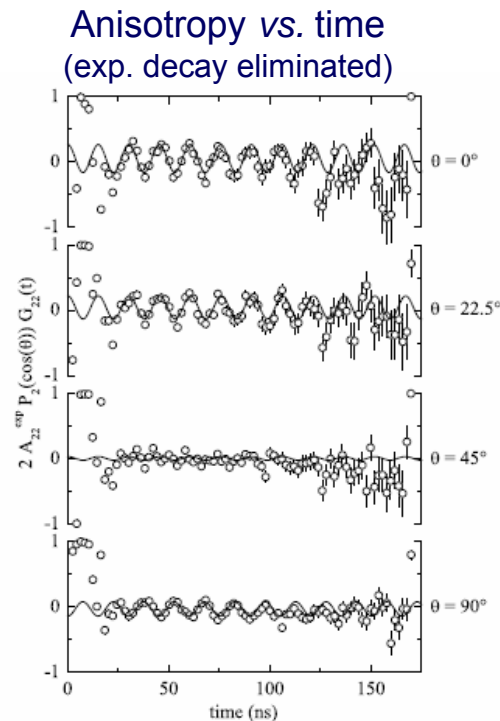
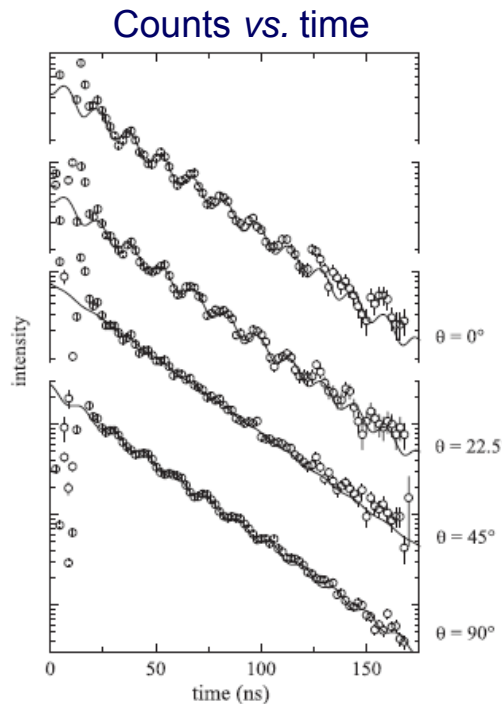
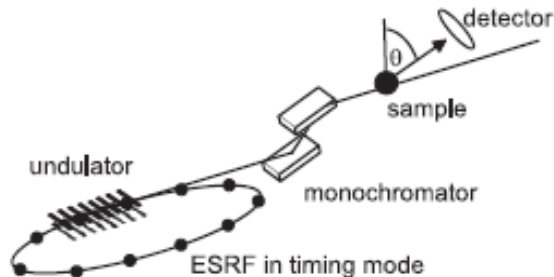


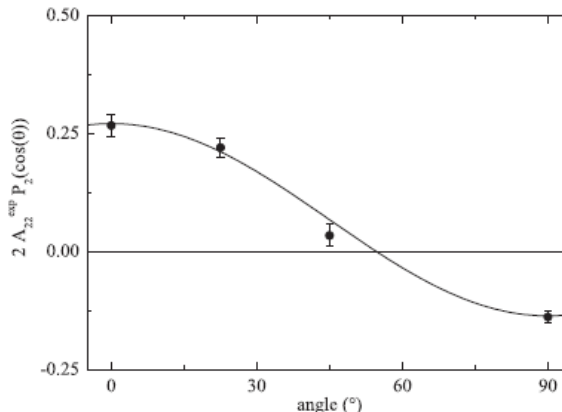
FIG. 8. Time evolution of the anisotropy $2A_{22}G_{22}(t)$ for several temperatures. The solid lines are fits by the theory given by Eqs. (3) and (10).

⁵⁷Fe in the molecular glass former dibutyl phthalate DBP doped with 5% mol of ferrocene FC enriched to 95% in ⁵⁷Fe.

Synchrotron-radiation-based perturbed angular correlations from ^{119}Sn



Angular dependence of $A_{22}G_{22}(t=0)$



Main areas of PAC research

Nuclear physics

- Nuclear moments

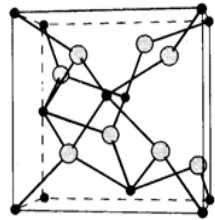
Condensed matter physics

- Magnetic properties of magnetically ordered systems
- Electric field gradients in non-cubic solids
- Dynamic processes: Atomic motion in solids, liquids , gases
- Phase transitions
- Defects in Solids
- Solid state reactions
- Biology; chemistry

Static QI in Solids: Phase identification and phase transformation

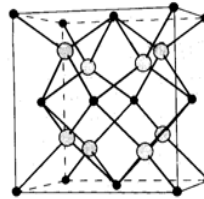
Example: ZrO_2

ZrO_2 phases



monoclinic

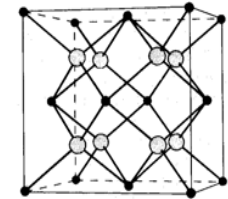
$v_q \neq 0$
 $\eta \neq 0$ $T \sim 1450$ K



tetragonal

$v_q \neq 0$
 $\eta = 0$

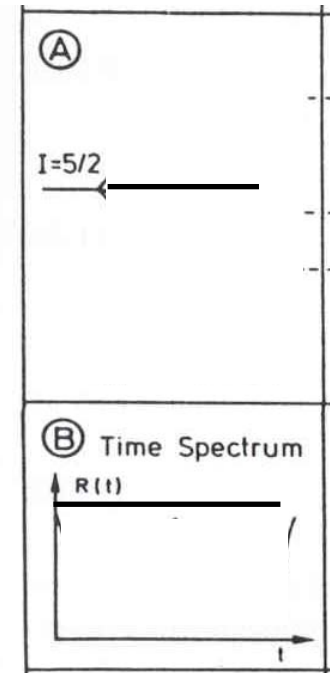
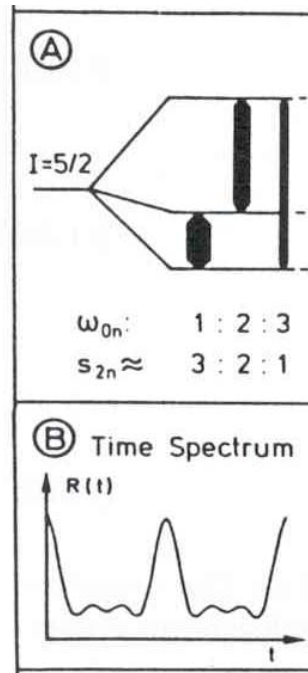
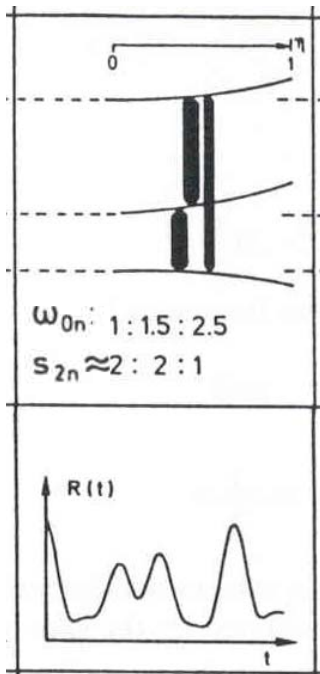
$T \sim 2150$ K



cubic, EFG = 0

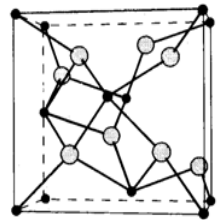
$v_q = 0$

QI and PAC spectra



Phase identification and phase transformation by QI - Example: ZrO₂

ZrO₂ phases

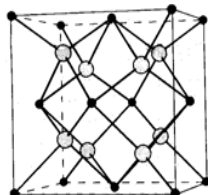


$$\nu_q \neq 0$$

$$\eta \neq 0$$

monoclinic

↓ T ~1450 K

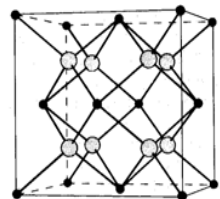


$$\nu_q \neq 0$$

$$\eta = 0$$

tetragonal

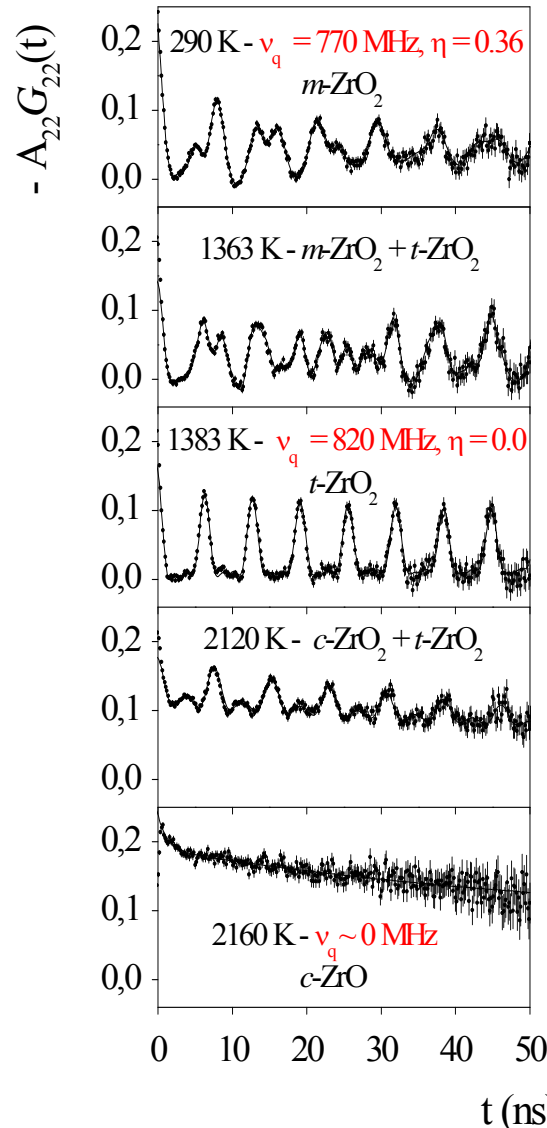
↓ T ~2150 K



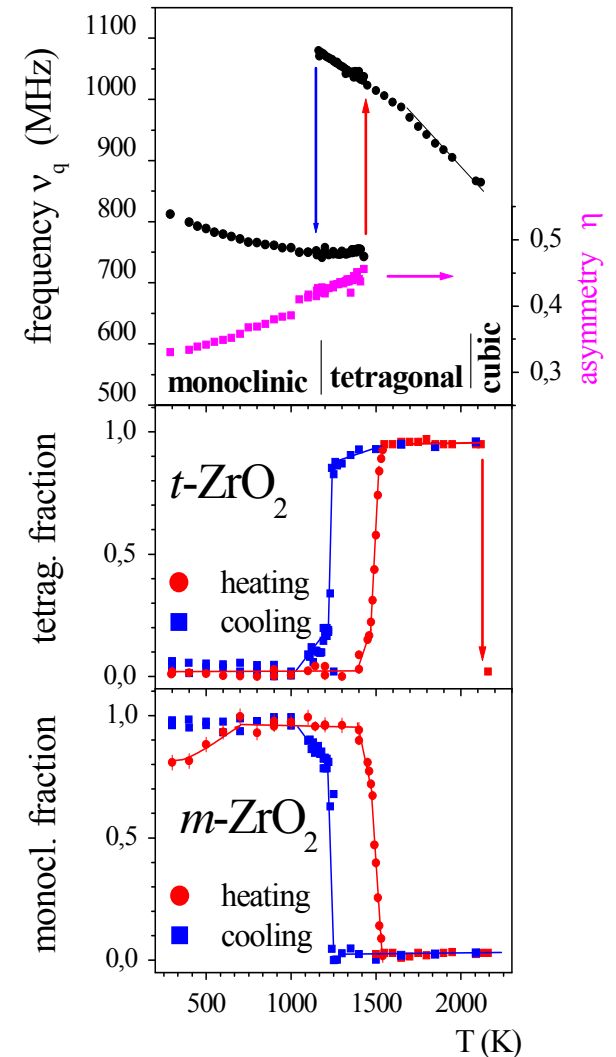
$$\nu_q = 0$$

cubic, EFG = 0

PAC spectra



Phase transformations



Static QI in solids:

Solid state reaction: Transformation of Zr metal into ZrB₂

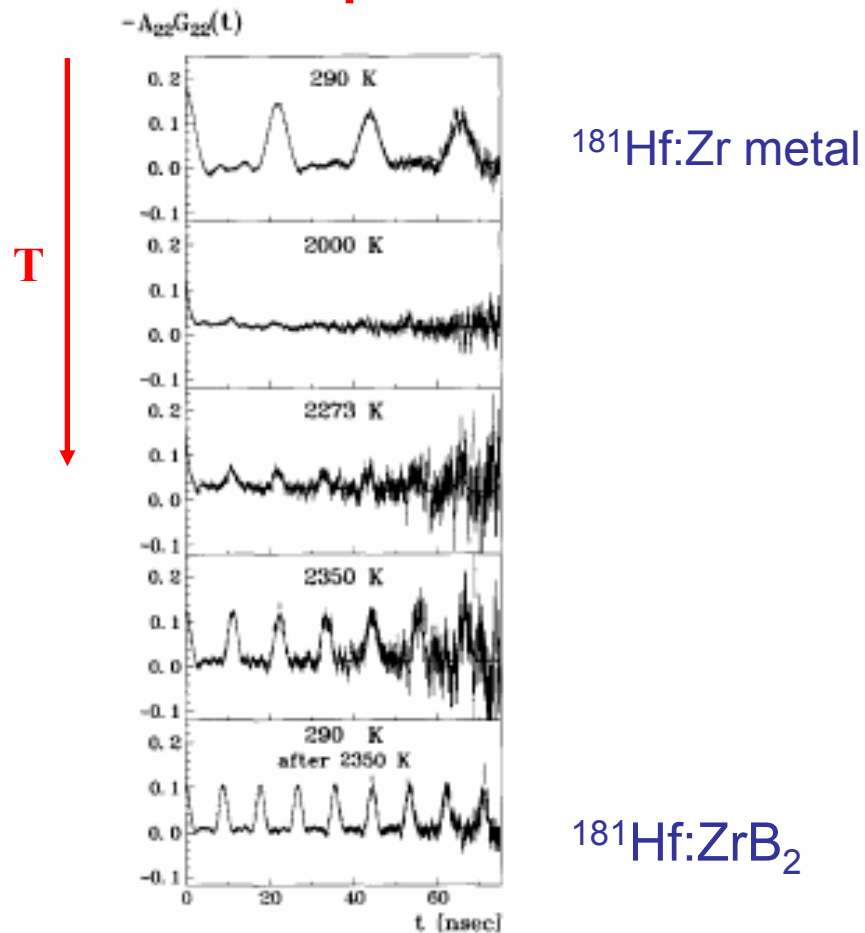
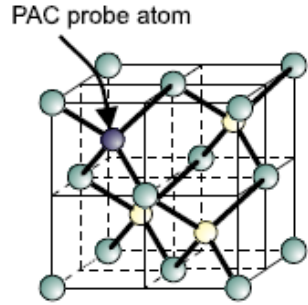
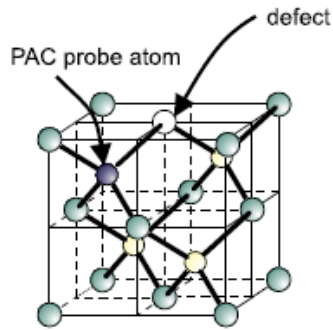
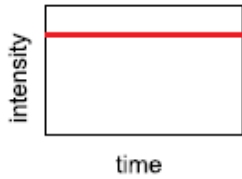


Fig. 4. PAC spectra of ¹⁸¹Ta in Zr metal, heated to 2350 K in a boron nitride crucible.

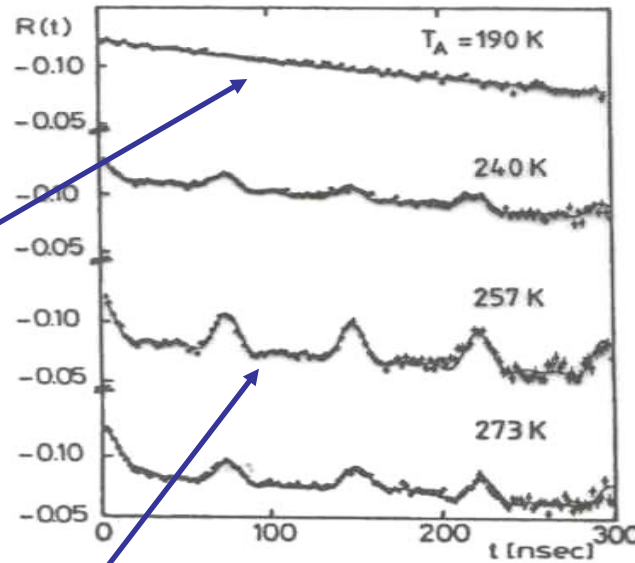
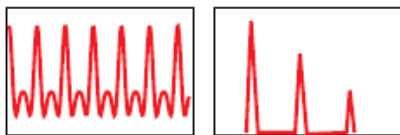
Static QI in solids: Defects in metals and semiconductors studied by TDPAC



cubic ↓ unperturbed



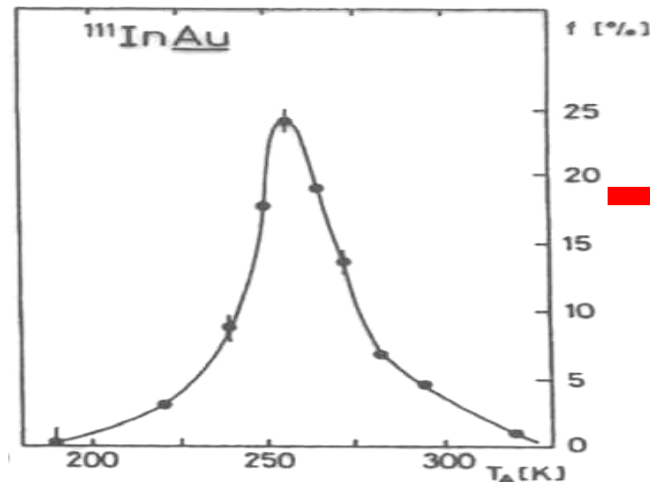
nn defect ↓ sharp QI



^{111}In in Au
e-irradiation
at low T

Subsequent
annealing

Probes with *nn* defect



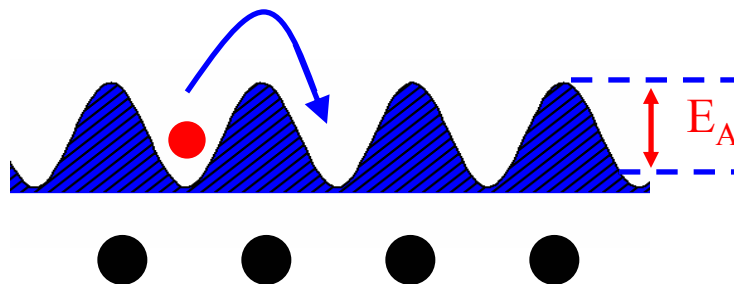
Defect migration
enthalpy

Probe-defect
binding energy

The perturbation of angular correlations by **dynamic QI**

Example: Hydrogen diffusion in solids

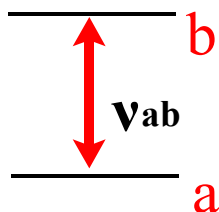
Thermally activated H diffusion



Activation energy

Residence time

$$\tau_R = \tau_R(0) \exp(E_A/k_B T)$$



Time dependent QI \rightarrow Nuclear relaxation; rate $R \approx \frac{v_f^2 \tau_R}{1 + (v_{ab} \tau_R)^2}$

$$R \approx \frac{v_f^2 \tau_R}{1 + (v_{ab} \tau_R)^2}$$

fast fluctuations:

$\tau_R \ll$ precession period $1/v_{ab}$

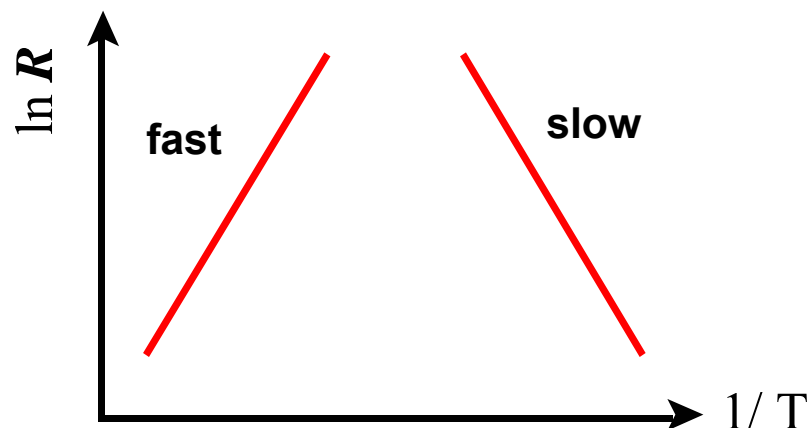
$$R \approx v_f^2 \cdot \tau_R \approx \exp(E_A/k_B T)$$

slow fluctuations:

$\tau_R \gg$ precession period $1/v_{ab}$

$$R \approx v_f^2 / \tau_R \approx \exp(-E_A/k_B T)$$

Arrhenius plot: $\ln R$ vs. $1/T$

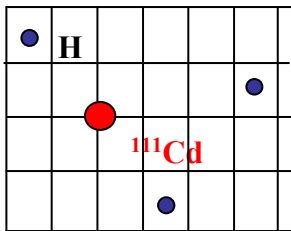


Hydrogen Diffusion studied by perturbed angular correlations

Characteristic times: Residence time τ_R and PAC time window $10 \text{ ns} \leq \Delta T \leq 1 \mu\text{s}$

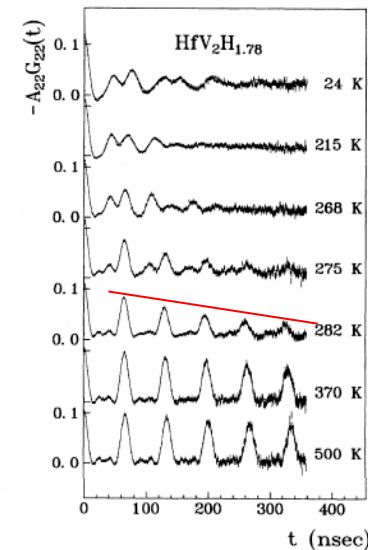
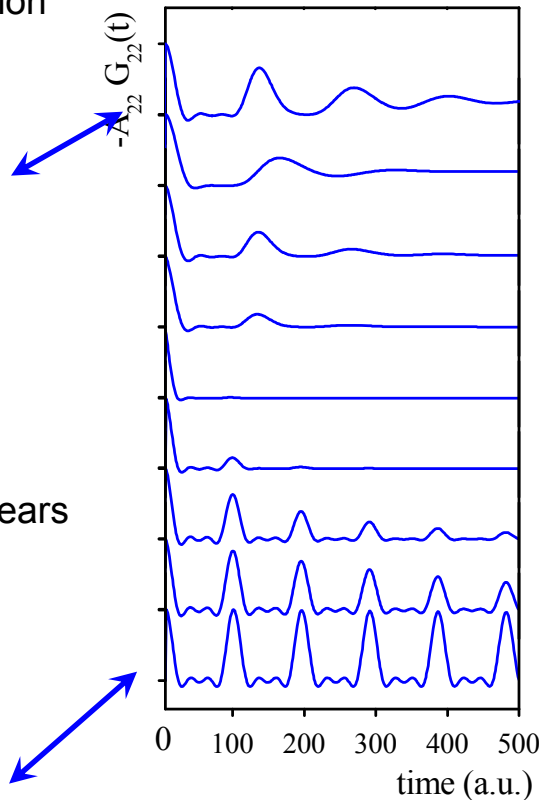
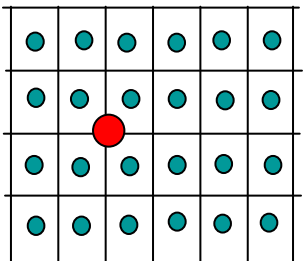
$\tau_R \gg \Delta T$:

(quasi-) static,
frequency distribution

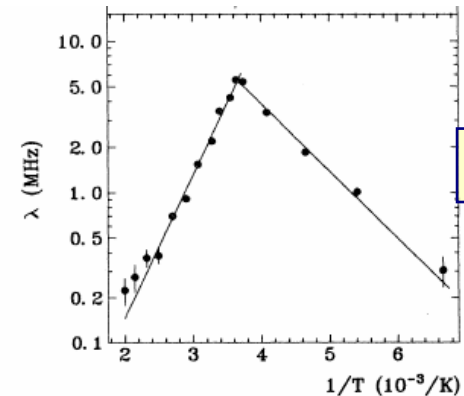


$\tau_R \ll \Delta T$:

fast fluctuations
time average appears
to be static



Arrhenius plot



Dynamic QI in solids: Reorientation jumps of ^{111}In in In_3La

M. Zacate, A. Favrot, G. Collins, PRL 92 (2004) 225901

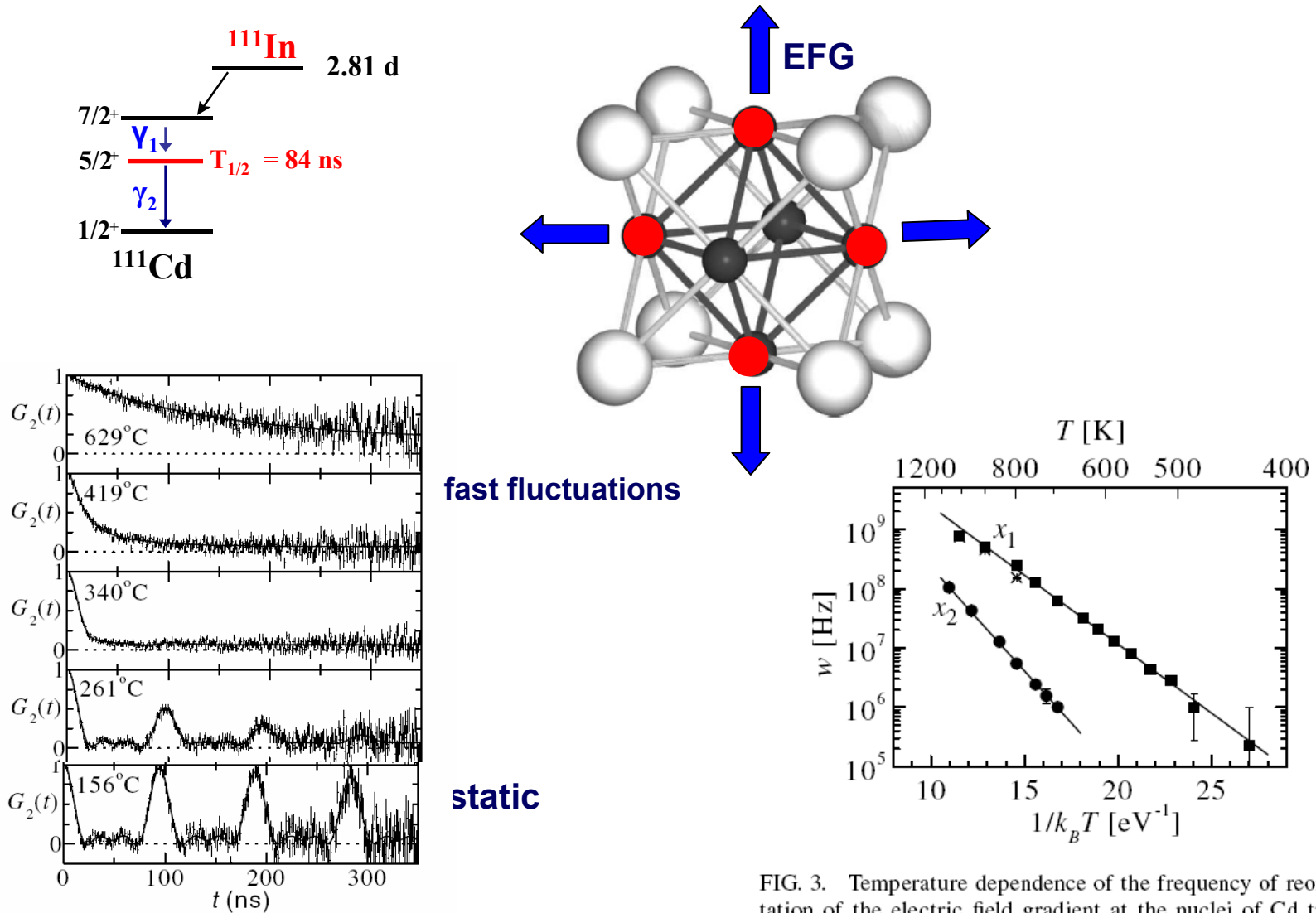


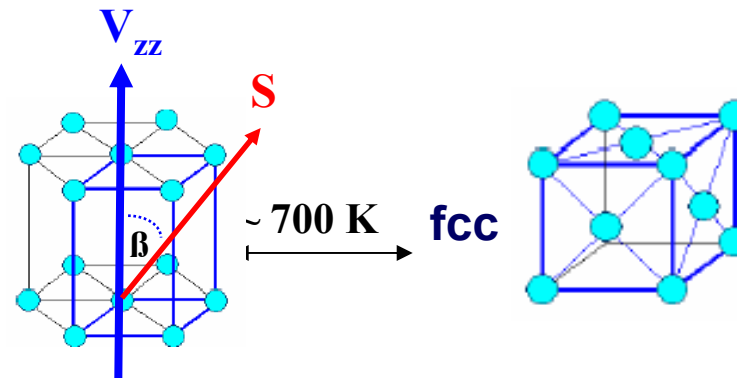
FIG. 2. Perturbation functions of ^{111}Cd tracer atoms in In_3La at the indicated temperatures.

FIG. 3. Temperature dependence of the frequency of reorientation of the electric field gradient at the nuclei of Cd tracer atoms caused by jumps on the In sublattice in In_3La . The lines indicate fits of data for the two different compositions, with symbols and labels defined in the text.

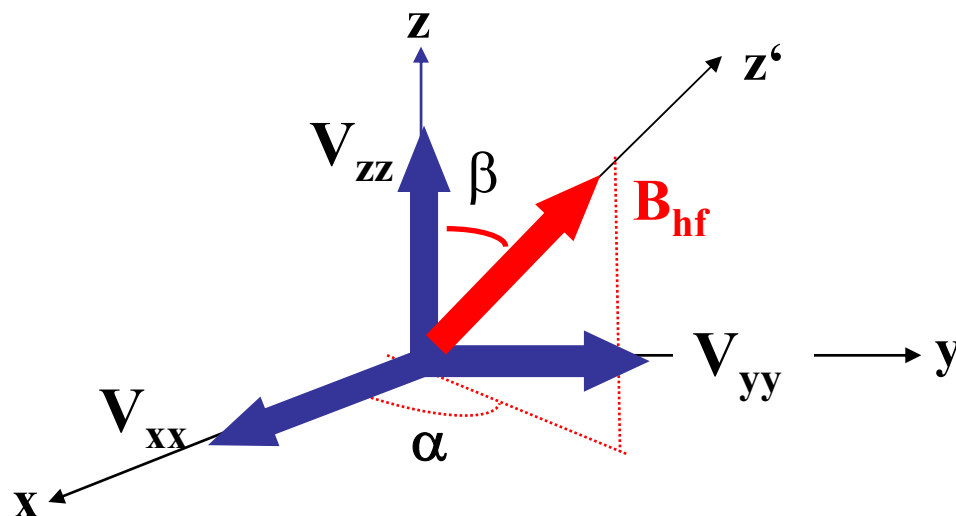
PAC study of magnetic properties

Example: ferromagnetic Cobalt

Cobalt: $T_c = 1390$ K, structure: hcp

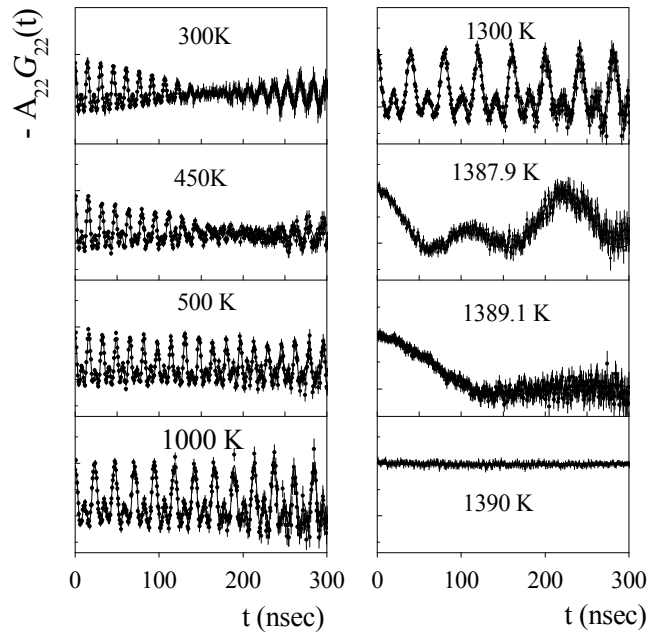


Combined magnetic + electric hfi

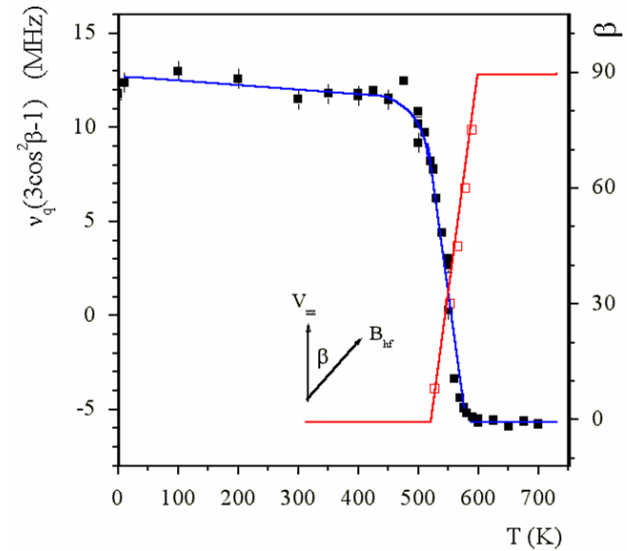


- $\nu_Q = eQV_{zz} / h$
- $\eta = \frac{V_{yy} - V_{xx}}{V_{zz}}$
- $\nu_M = g\mu_B B_{hf} / h$
- Euler angles β, γ

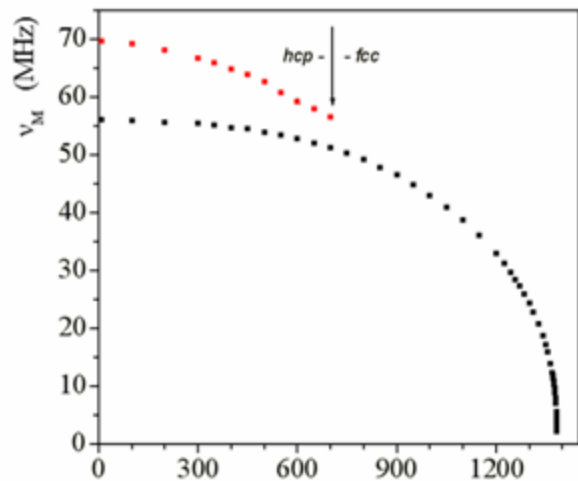
PAC spectra of ^{111}Cd in Co



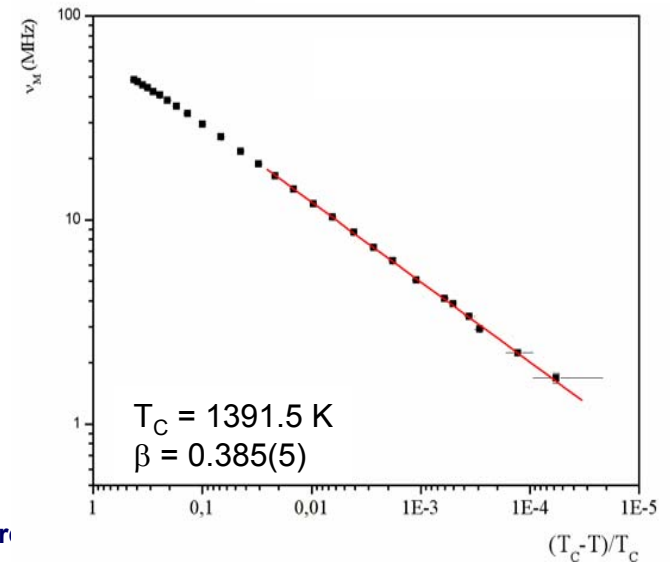
Spin reorientation



Temperature dependence of v_M



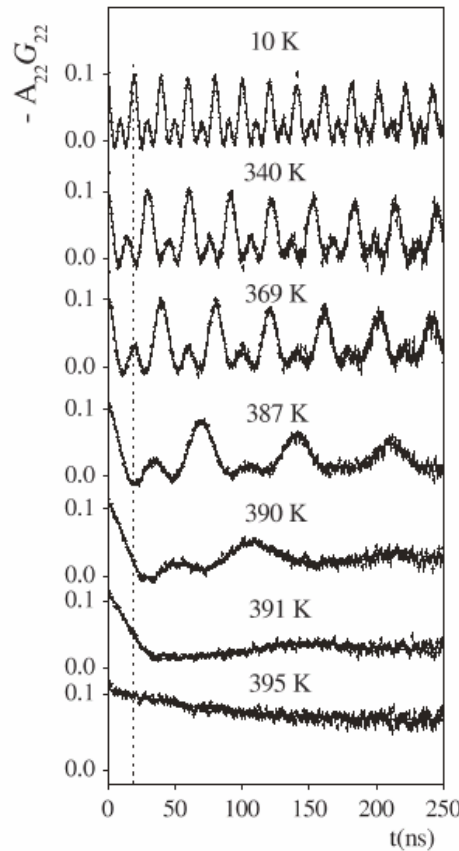
critical exponent: $v_M(T) = v_M(0)(1 - T/T_C)^\beta$



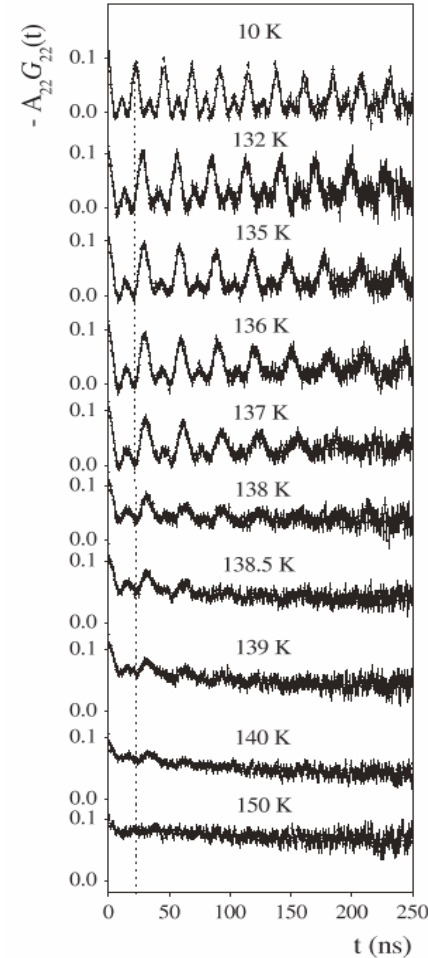
Phase transitions of $R\text{Co}_2$

studied by measurement of the temperature dependence of the magnetic hyperfine field

Rare earth = Pr, Nd, Sm, Gd, Dy, Ho, Er, Tm

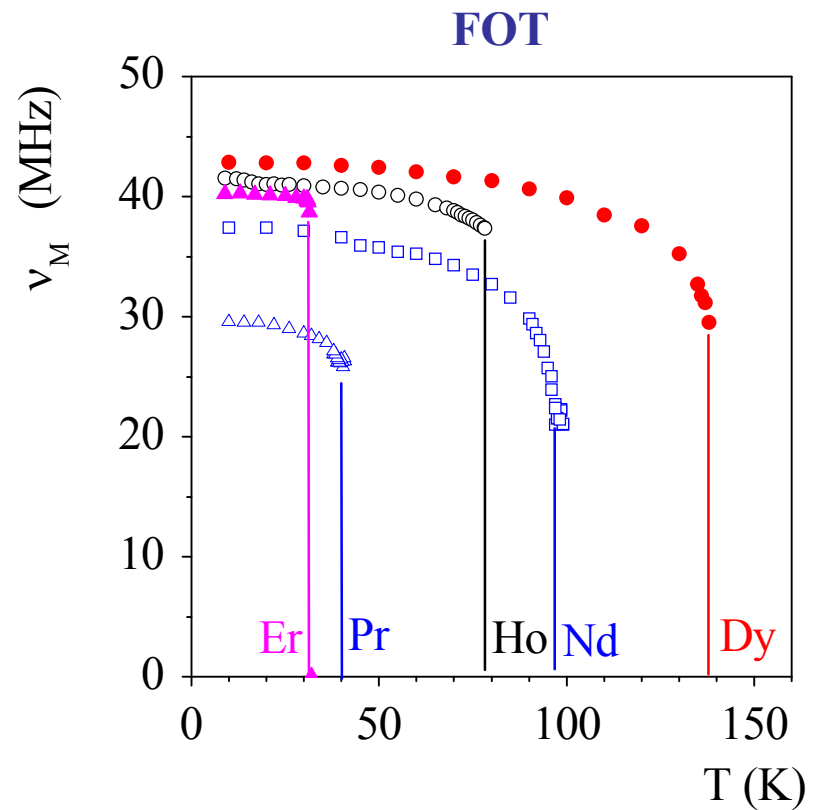
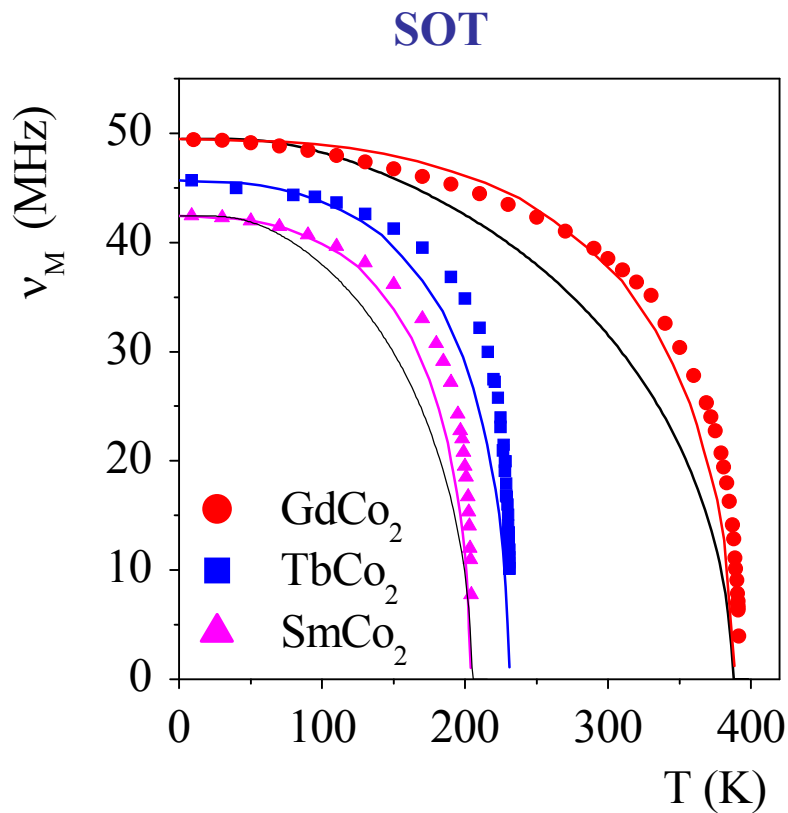


GdCo_2
**Second-order
Transition
SOT**



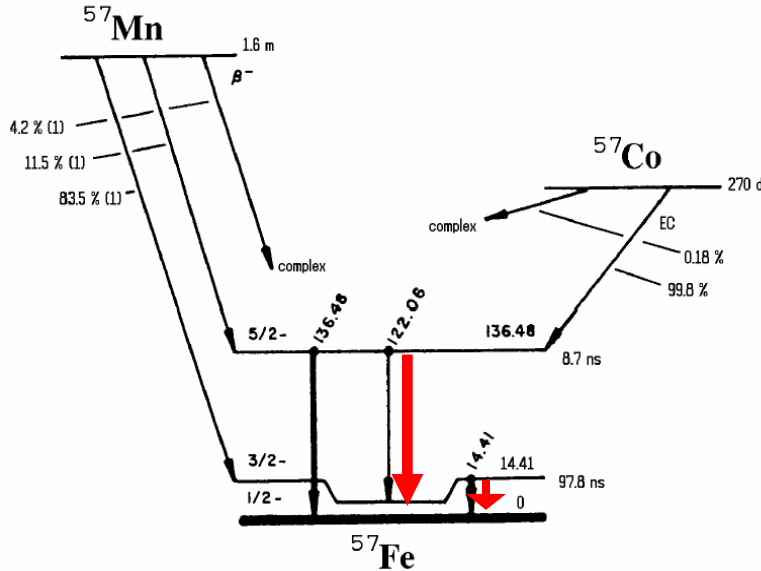
DyCo_2
**First-order
Transition
FOT**

The order of the magnetic phase transitions of $R\text{Co}_2$ deduced from the magnetic hyperfine field at ^{111}Cd



Time-Differential Perturbed Angular-Correlation Experiment for ^{57}Fe in a Ni Host, and a Comparison with the Mössbauer Effect*

C. HOHENEMSER, R. RENO, H. C. BENSKI, AND J. LEHR†

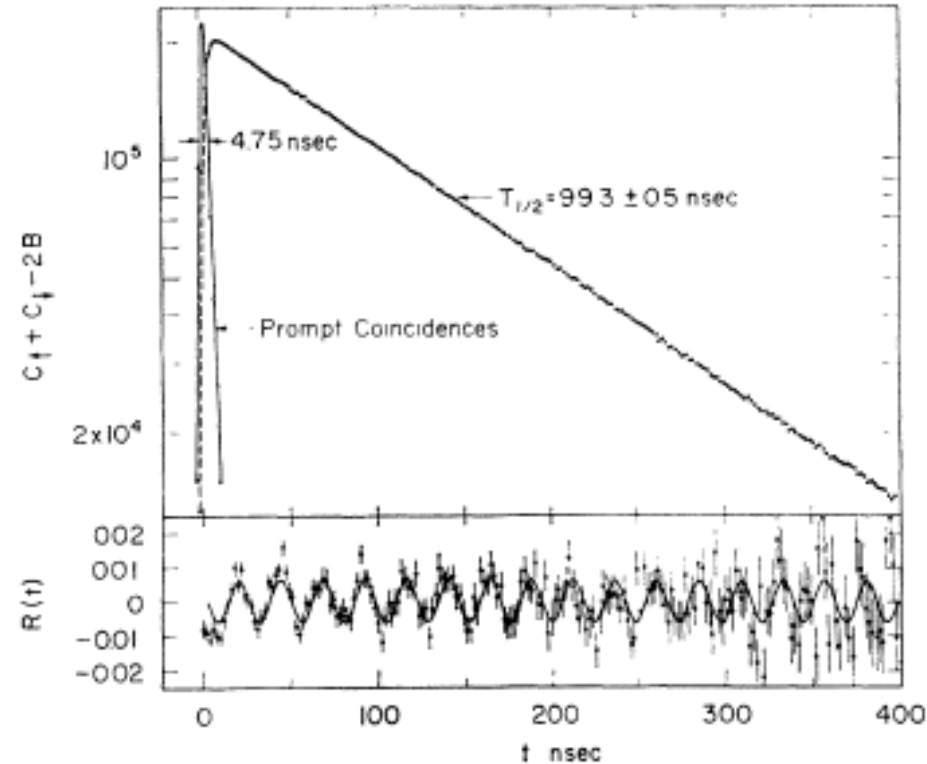
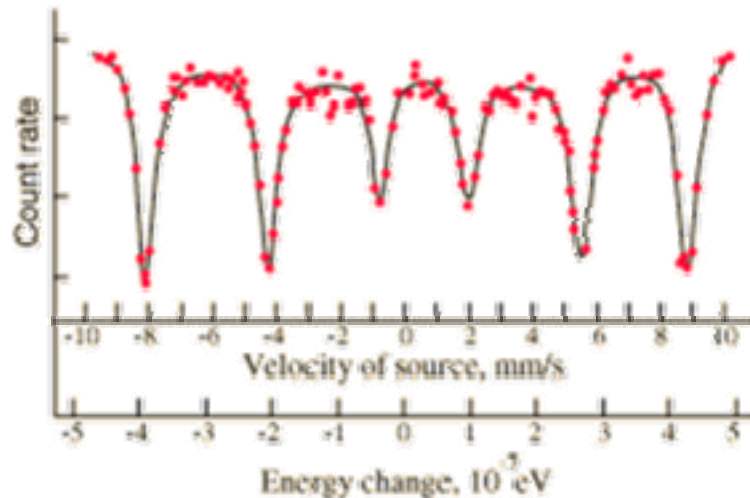


PAC source: ^{57}Co in Ni

$|B_{hf} (^{57}\text{Fe:Ni})| = 267.8(2.7) \text{ kG}$

Mössbauer: 265(5) kG

$|B_{hf} (^{57}\text{Fe}:\alpha\text{-Fe})| = 330 \text{ kG}$



Comparison PAC – Mössbauer, NMR, NQR, NO, SH....

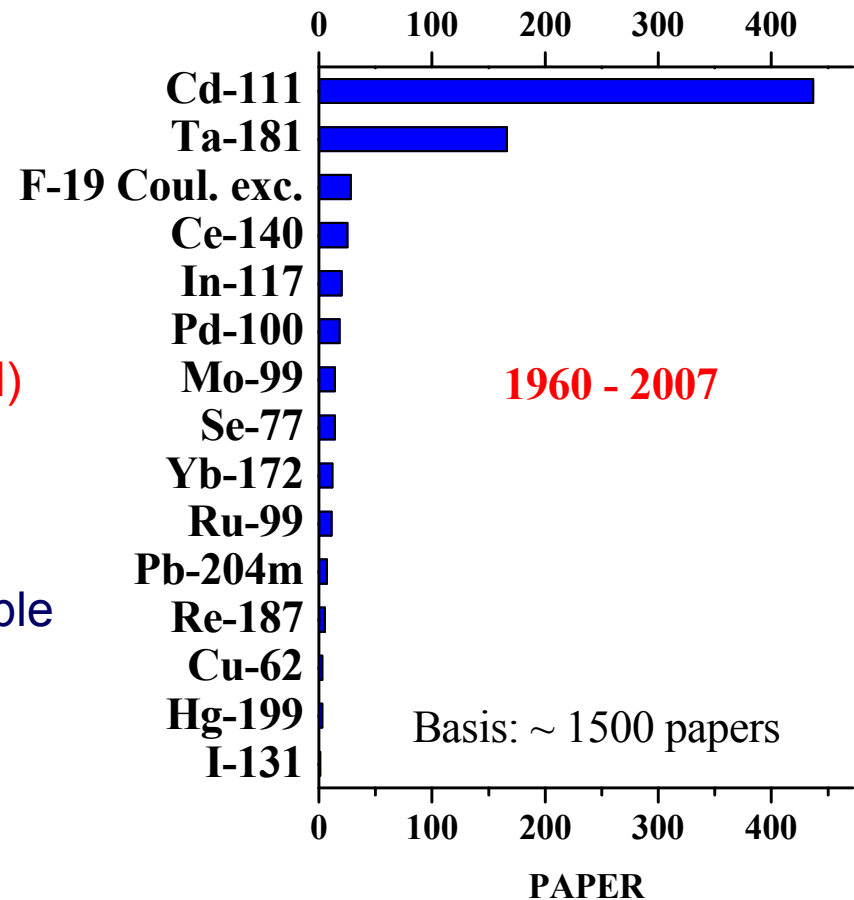
Advantages of PAC:

- Any temperature
- Any environment (solid, liquid, gas)
- Low concentration of probe nuclei:
 $10^{-12} - 10^{-6}$
- No restriction to low E_γ
- Small samples: 1-100 mg
- No external field or rf field required

Comparison PAC – Mössbauer, NMR, NQR, NO, SH,...

Disadvantages of PAC

- Limited number of probes for laboratory experiment
- Source preparation (Radiochemistry installations required)
- Legal constraints
- Probe mostly an impurity in the sample
- Complex electronic set-up



Global PAC Activity

